

Design of peptides interfering with iron-dependent regulator (IdeR) and evaluation of *Mycobacterium tuberculosis* growth inhibition

Himen Salimizand¹, Saeid Amel Jamehdar^{1,2}, Leila Babaei Nik³, Hamid Sadeghian^{2,4*}

¹ Department of Microbiology and Virology, School of Medicine, Mashhad University of Medical Sciences, Mashhad, Iran

² Antimicrobial Resistance Research Center, Avicenna Research Institute, Mashhad University of Medical Sciences, Mashhad, Iran

³ Tuberculosis Reference Center, Dr Shariati Hospital-Mashhad University of Medical Sciences, Mashhad, Iran

⁴ Department of Laboratory Sciences, School of Paramedical Sciences, Mashhad University of Medical Sciences, Mashhad, Iran

ARTICLE INFO

Article type:

Original article

Article history:

Received: Oct 3, 2016

Accepted: May 25, 2017

Keywords:

IdeR

Inhibitor

Modeling

Mycobacterium –

Tuberculosis

RT-PCR

ABSTRACT

Objective(s): Tuberculosis (TB), a disease caused by *Mycobacterium tuberculosis* (*Mtb*), stayed a global health thread with high mortality rate. Since TB has a long-term treatment, it leads high risk of drug resistant development, and there is an urgent to find new drugs. The aim of this study was designing new inhibitors for a new drug target, iron dependent regulator, IdeR.

Materials and Methods: Based on the interaction most populated amino acids of IdeR to the related gene operators, 50 short peptides were modeled. Bonding affinity of short peptides toward DNA were studied by docking. Top 10 best predicted bonding affinity were selected. DNA binding assay, microplate alamar blue assay, colony counting, quantitative real time- PCR (qRT-PCR) of IdeR corresponding genes, cell wall-associated mycobactin and whole-cell iron estimation were done to prove the predicted mechanism of *in silico* potent constructs.

Results: Amongst the 10 synthesized short peptide candidates, glycine-valine-proline-glycine (GVPG) and arginine-proline-arginine (RPR) inhibited *Mtb in vitro* at 200 μ M concentration. qRT-PCR showed *mbtB* 58-fold over expression that resulted in *Mtb* growth inhibition. Cell wall-associated mycobactin and whole-cell iron estimation confirmed the results of qRT-PCR.

Conclusion: We introduced two new lead compounds to inhibit *Mtb* that are promising for the development of more potent anti-tubercular therapies.

► Please cite this article as:

Himen Salimizand, Saeid Amel Jamehdar, Leila Babaei Nik, Hamid Sadeghian. Design of peptides interfering with iron-dependent regulator (IdeR) and evaluation of *Mycobacterium tuberculosis* growth inhibition. Iran J Basic Med Sci 2017; 20:722-728. doi: 10.22038/IJBMS.2017.8859

Introduction

Tuberculosis (TB), a disease caused by *Mycobacterium tuberculosis* (*Mtb*), stayed a global health thread with high mortality rate. In 2016, it is estimated that 10.4 million new TB cases were developed and 1.4 million died from TB (1). High rate of TB in developing countries, low quality of education and long-term treatment are factors that lead risk of drug resistant *Mtb*. Indeed, 3.3% to new TB cases and 20% of treated cases have developed multi-drug resistant TB (MDR-TB). The problem has worsened with arising of extensively drug-resistant TB (XDR-TB) that presented in 9.7% of MDR-TB cases (1). Whereas there is an urgent need to find new drugs, it has only two new drugs, bedaquiline and delamanide, have been approved after five decades (2, 3).

Efforts to find new drug targets in *Mtb* have resulted in identifying key proteins that are promising to defeat TB (4). Global regulators that are

central in biological metabolisms are of interest since there are different genes regulated by them (5). Iron dependent regulator protein, IdeR, nominated Rv2711, as repressor/inducer controls 51 genes that are critical for *Mtb* metabolism, especially those that are related to iron-dependent genes expression, iron metabolism, and oxidative stress responses (5). Of which, *mbtB* and *bfrB* are more affected due to their straight role in uptake and storage of iron, respectively (5, 6).

Iron is involved in essential cellular functions, but very limited in the environment. However, due to generating toxic reactive oxygen species (ROS) in aerobic respiration in the Fenton reaction (7) controlling intracellular concentration is critical to the organism. IdeR and under-regulated genes play important roles in this issue. Since IdeR protein is crucial to *Mtb*, *ideR* mutation, non-functional protein and disordering function kills bacterium (6).

Crystallographic studies on IdeR revealed the

*Corresponding author: Hamid Sadeghian. Antimicrobial Resistance Research Center, Avicenna Research Institute, Mashhad University of Medical Sciences, Mashhad, Iran. Tel: +98-51-38002214, Fax: +98-51-38828564; email: sadeghianh@mums.ac.ir

protein-protein and protein-DNA interactions of this protein, in detail (8). In the case of monomer construction, three structural domains are considered, that could explain the biological function of this protein. Domains were assumed to be DNA-binding domain (DBD), includes amino acid no. 1 to 74, dimerization domain (DD), 75 to 140, and SH3-like domain, consisting of residues 151 to 230. However, complete functional activity of IdeR occurred when it forms dimers, but in the presence of iron, that interact to the conserved region on DNA (8). Therefore, successful inhibition of dimer formation or inhibiting the interaction of IdeR to related sequence of DNA may result in non-expression or over-expression of related genes. In this study, we have focused on the *in silico* designed competitors that intercept IdeR to DNA.

Materials and Methods

Designing constructs

The structures of short peptides were drawn by ChemDraw Ultra 8.0. The two dimensional (2D) structures of peptides were exported to HyperChem 8 software. To simulate the three dimensional (3D) structures, conformational analysis has been performed by MM+ (RMS gradient=0.05 kcal mol⁻¹) and AM1 methods (convergence limit=0.01; Iteration limit=50; RMS gradient=0.05 kcal mol⁻¹; Polak-Ribiere optimizer algorithm) (9).

For docking analysis, the 33-mer DNA sequence of iron box and constructs were submitted to AutoDock software (AutoDock Tools, V. 1.5.6).

The docking regions of the DNA were defined by considering Cartesian chart -5.534, -0.100, and 3.698 as the central of a grid size with 60, 60 and 60 points in X, Y and Z axis. Lamarckian genetic algorithm Parameters (GALS) were used for generating the docking parameter files. The number of generations and maximum number of energy evaluations was set to 200 and 2,500,000, respectively. The root-mean-square deviation tolerance (RMSD) of 2.0 Å was considered to cluster 200 docked complexes. Calculations were outputted as free energy of binding (ΔG_b). Estimated dissociation constant (K_d) was calculated by using of this equation: $\Delta G_b = 2.3RT \log K_d$ ($K_d = 1/K_b$). Peptides were ordered with >95% purity (MIMOTOPES, Australia). Then, they were subjected for further investigations (Figure 1).

Modified DNA binding assay

To evaluate the affinity of constructs to DNA duplex, a competitive assay based on DNA/Methyl green displacement was performed (10).

A 33-mer oligonucleotide of both forward and reverse strands of the *mbtA-mbtB* operator sequences was obtained at the highest available molarity (Macrogene, Korea). Duplexes were generated through mixing equimolar amounts of

both strands, by heating to 95 °C for 5 min, and slowly cooling. To confirm duplex formation a 7% polyacrylamide gel was used to run 1 µl of mixture.

Methyl green (MG) (Sigma), at the final concentration of 10 µM was mixed with 1 µM of DNA duplex and remained at least 15 min at room temperature before adding constructs. Constructs at 11 concentrations, 800, 400, 200, 100, 50, 25, 12, 6, 3, 1 and 0.5 µM, were added to the DNA/MG mixture and the volume adjusted to 100 µl with distilled water per well. DNA/MG, construct/DNA, construct/MG and MG solely were separately embedded in distinct wells to unravel the discrepancies. Experiments were repeated at least in triplicate. A non-binding flat bottom clear ELISA microplate (Greiner Bio One, Austria) were used to spectrophotometric assay. Inoculated plates were left 24 hr at darkness and results were measured spectrophotometrically (BioTek, Winooski, VT, USA) at 630 nm wavelength. IC₅₀ of each construct calculated based on the concentration that was required to decrease 50% of initial absorbance of DNA/MG complex by using of binding-competitive equation in PRISM 6.0. (11).

Bacterial strain and media

Mtb strain H37Rv ATCC 27294 was used in all of the experiments. Middlebrook 7H9 broth (Himedia, India) was used as high-iron medium (h7H9). To assay *Mtb* growth under low-iron conditions (1 µM), we reconstitute 7H9-based composition medium (r7H9) by adding 1 µM of iron in the form of FeCl₃. The amount of iron was determined by atomic absorption spectroscopy. Both of media were supplemented by 10% ADC (Fluka), 0.2% glycerol, 0.05% Tween-80 and 0.085% NaCl. All chemicals were provided from Sigma.

Microplate alamar blue assay (MABA) and colony counting

The microplate alamar blue was used to assess sensitivity of *Mtb* to the constructs (12). Briefly, 10⁶ colony forming units (CFUs) of *Mtb* cells were inoculated in 1 ml of h7H9 and r7H9 that at serial dilution manner, contained 800, 400, 200, 100, 50, 25, 12, 6, 3, 1 and 0.5 µM concentration of constructs. After one week incubation, 100 µl of media transferred to 96-well U-bottom microplates (Greiner Bio One, Austria) and 20 µl of 0.01% resazurin was added to each well. After 24 hrs results were recorded. In addition, 100 µl of initial inoculated broth mediums were subjected to 10⁻³ dilution, and 50 µl of diluted bacteria were seeded into LJ (Löwenstein-Jensen) medium for colony counting. Experiments were done in triplicates. After three weeks incubation colony forming units of *Mtb* were counted. Construct-free bacterial inoculated broth media, h7H9 and r7H9, were considered as initial growth controls.

Table 1. Different processes to find out the interaction of IdeR-construct-DNA. In the processes of 9 and 10 *Mtb* cells were not transferred to the second medium, and cells remained in the initial medium to the end of incubation. Experiments were repeated three times. Abbreviations: r7H9, reconstituted 7H9; h7H9, hi-iron 7H9; compd., compound

Process	Initial medium	Second transferred medium
1	r7H9	h7H9-Compd.
2	r7H9	r7H9-Compd.
3	h7H9	h7H9-Compd.
4	h7H9	r7H9-Compd.
5	r7H9-Compd.	r7H9
6	r7H9-Compd.	h7H9
7	h7H9-Compd.	r7H9
8	h7H9-Compd.	h7H9
9	r7H9-Compd.	-
10	h7H9-Compd.	-

To analyze the exact function of IdeR-construct-DNA interaction in different iron-content media, we defined several processes (Table 1). *Mtb* cells were cultured in r7H9 and h7H9, with and without constructs. After 48 hrs of incubation in 37° C, cells were washed three times by phosphate buffer saline (PBS), and then transferred to the second medium.

Quantitative real-time PCR

Mtb cells from different processes (Table 1) were subjected to qRT-PCR. Total RNA extraction, cDNA synthesis and quantitative reverse transcription-PCR (RT-PCR) were performed as previously described by Pandey *et al.* using primers targeting *mbtB* and *bfrB* of *Mtb* (6). qRT-PCR was performed by the Rotor-Gene 6000 instrument (Corbett Life Science, Valencia, CA) using Real-Time SYBR green 2x Master Mix (Parstous, Iran) in triplicates. The results were normalized to the amount of 16S rRNA and were calculated by 2^{-ΔΔCT} Method (13).

Cell wall-associated mycobactin and whole-cell iron estimation

To assess inhibitory role of constructs on IdeR function, cell wall-associated mycobactin and whole cell iron were measured. The prior, as the consequence of *mbtB* expression, and the latter, as the outcome of *bfrB*, could explain the efficacy of each construct, respectively.

Cell wall-associated mycobactin was determined by a simple method, as described by Schwyn *et al.* (14). *Mtb* cells from processes (Table 1) were washed three times by PBS, then, were subjected to overnight chloroform-ethanol (1:1) protein extraction. A drop of FeCl₃ saturated in ethanol was added, and, the optical density at 450 nm was observed.

Intracellular iron content was measured as previously described by Dragset *et al.* (15). Briefly, *Mtb* was cultured in h7H9 and r7H9 with construct. After 48 hr bacteria were centrifuged and three times washed with PBS. After acid nitric digestion, H₂O₂ was added to the mixture; then diluted with 2 ml water, metal content was scaled by atomic absorption spectroscopy (Analyst 300; PerkinElmer, Foster City, CA, USA).

Cellular toxicity assay

To found the cellular toxicity of constructs MDCK cell line was used. The number of viable cells was measured via 0.25% Trypan Blue on haemocytometer. Cells were cultured in Dulbecco's Modified Eagle's Medium (DMEM) (Sigma) culture medium which supplemented by 10% heat-inactivated fetal bovine serum (FBS) (Gibco), 100 mg/ml streptomycin (Sigma), 100 unit/ml penicillin (Sigma) and 2 mM L-glutamine (Sigma). A total of 5.0×10³ cells were seeded in each well of 96-well microplate that contained 100 μL of medium and incubated overnight at 37 C in 5% CO₂. Then, with a 100 μl of 0.25% FBS culture medium containing 800 μM of constructs the cell culture medium replaced, and incubated 24 hr at 37 °C in 5% CO₂. About 20 μl of 0.01 % of resazurin was added to each well and incubated in the same conditions again. The results were recorded observationally 24 hr later. Experiments were done in triplicate for all constructs. Furthermore, bacterial strains including *Escherichia coli*, *Staphylococcus aureus* and *Pseudomonas aeruginosa* were studied to find the sensitivity of these strains to constructs at the concentration of 800 μM.

Results

Modeling of the constructs

According to the crystallographic analysis of IdeR (PDB entry: 1U8R), the interaction of the DBD of IdeR, few residues directly abutted on the iron box of DNA promoters. Predominant amino acids in this region are valine (V), alanine (A), glycine (G), threonine (T), proline (P), arginine (R), serine (S), glutamine (Q) and asparagine (N). Among them R47, R50, Q43, S37 and Q36 have hydrogen bonds with the nucleotides of DNA iron box (Figure 1).

According to these data, 50 constructs with three to four residues from the aforementioned amino acids were designed and their binding potency towards DBD were evaluated by AutoDocTools 4.2 software. The docking results were further analyzed to find a binding conformer from each cluster with the lowest K_d (estimated DNA-ligand dissociation constant), and finally, the average of the aforementioned K_d were calculated and named as K_d* for each of the synthetic peptides. Constructs that had K_d* lower than 100 μM

Table 2. Characteristics comparison of construct's *in silico* and *in vitro*. Bolded constructs showed anti-mycobacterial activity. Abbreviations: K_d^* , average of lowest K_d ; MABA, microplate alamar blue assay; MIC, minimum inhibitory constant

Structure	K_d^*	Best predicted K_d calculated by AutoDoc (μM)	DNA/MG spectrophotometric IC_{50} (μM)	MABA MIC (μM)	Colony counting
GVPG	-5.28	2.9	4	200	78.10^3
SGP	-4.73	33	128	>800	$>10^6$
PTV	-4.35	38.75	147	>800	$>10^6$
PRP	-5.81	2.55	10.2	>800	$>10^6$
SPR	-5.2	17.83	20	>800	$>10^6$
SRP	-5.24	9.74	101	>800	$>10^6$
RPR	-5.78	2.79	2.8	200	55.10^3
PRG	-5.04	6.77	8	>800	$>10^6$
QTQ	-4.00	60.72	316	>800	$>10^6$
PPQ	-5.22	103.6	158	>800	$>10^6$

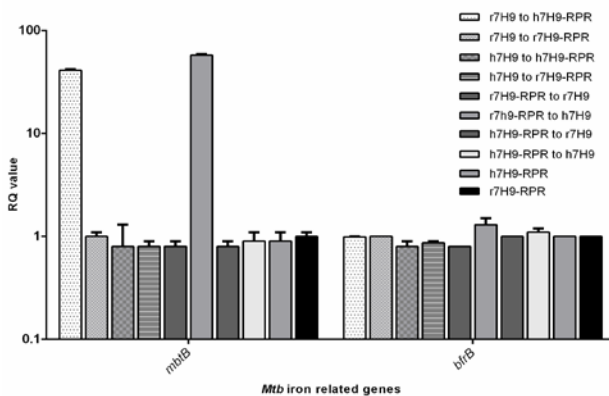


Figure 5. Changes of the expression level of iron-responsive genes, *mbtB* and *bfrB*, of *Mtb* cells grown in r7H9 and h7H9, with or without construct RPR. Construct GVPG had the same results (data not shown). The relative transcript levels of two iron-responsive genes (*mbtB* and *bfrB*) were measured by quantitative RT-PCR. Results from three experiments were calculated by $2^{-\Delta\Delta\text{CT}}$. RQ (relative quantification) values are presented in Log_{10}

qRT-PCR of *mbtB* and *bfrB*

Constructs were designed to interfere with iron hemostasis, and, they were expected to up or down-regulate related genes. Real time results showed that constructs GVPG and RPR at the concentration of 200 μM could affect the expression of *mbtB* genes, where *Mtb* cells were grown in r7H9 and h7H9 (Figure 5). A 41-fold increase in expression of *mbtB* was seen in the condition that *Mtb* was cultured in depleted iron medium, r7H9, followed by growth in constructs containing high iron medium, h7H9-compd. Constructs GVPG and RPR showed the same level of increase in expression of *mbtB*. Furthermore, 58-fold increase in *mbtB* expression were observed where *Mtb* cells were grown initially in r7H9 containing constructs (r7H9-compd) and then transferred to h7H9 medium. The expression level of *bfrB* was not affected by constructs, grown or transferred, neither r7H9 nor h7H9.

Cell wall-associated mycobactin and wholecell iron estimation

To ascertain IdeR dysfunction, we analyzed the cell wall-associated mycobactin and wholecell iron content, as the result of *bfrB* and *mbtB* expression level.

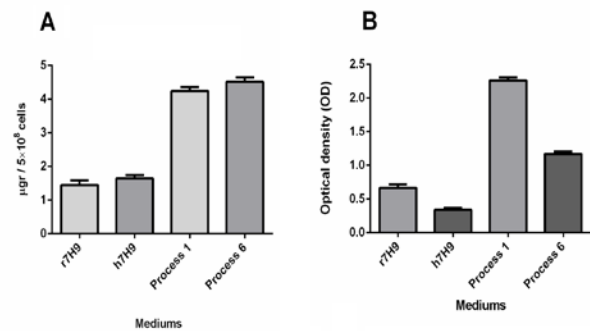


Figure 6. Wholecell iron and cell-associated mycobactin after treating with the 200 μM concentration of construct RPR. Construct GVPG had the same results (data not shown). Results were collected from 5×10^8 CFU of *Mtb* cells. A) Wholecell iron of *Mtb* cells in media, r7H9 and h7H9, processes 1 and 6. B) Cell-associated mycobactin harvested from *Mtb* cells cultured in media, r7H9 and h7H9, r7H9 and h7H9, processes 1 and 6

As the same as real-time PCR results, constructs GVPG and RPR at the concentration of 200 μM could only change iron and mycobactin content of those *Mtb* cells that grown in r7H9 medium and transferred to h7H9. No differences were observed in iron and mycobactin content in *Mtb* cells grown under the other conditions (Figure 6).

Cellular toxicity assay

MDCK cell line growth did not inhibited under 800 μM of constructs. As the constructs were indeed short peptides, it could be expected that, they did not affect mammalian cell growth. Additionally, bacterial strains were not susceptible to the constructs at the concentration of 800 μM (data not shown).

Discussion

Iron is crucial metal for *Mtb* survival, but excess amount is toxic. Hence, iron hemostasis is strongly controlled. Therefore, iron metabolism, and, in particular, IdeR has the potential to be considered as new drug target. In this study we targeted the binding site of IdeR holo-protein to DNA operator through mimicking DBD of IdeR to DNA, in the form of short peptides.

According to the processes presented in Table 1, only the processes were successful that *Mtb* cells were in the low-iron 7H9, r7H9, and then transferred to high-iron 7H9, h7H9. In iron limited conditions, like intracellular conditions, IdeR subunits cannot assemble. In the other hand, constructs entered, and when iron increases, assembled IdeR unable to regulate *mbtB*. Therefore, it up-regulates and cellwall associated mycobactin increased. Consequently, intracellular iron increased and overloaded that harms the cell through Fenton reaction. However, *bfrB* regulation, in comparison to the normal conditions, is not affected by the constructs (Figure 6). It can be explained in the way that, when cell is in iron deplete conditions, IdeR does not attached to the *bfrB* operator. But, when the iron increased in the presence of constructs, IdeR still cannot attach to the *bfrB* operator, and the expression level of this gene remained as the same as iron limited conditions. The lack of bacreioferritin, as the product of *bfr* gene, leads to lack of control over the iron storage, which leads to increasing free iron in the cell. Free oxygen radicals as the result of Fenton reaction damage biomolecules.

In the other study 92 components and 85 protein-protein interactions in iron hemostasis of *Mtb*, as a modeled system, were analyzed. They have found the importance of IdeR in *Mtb* as a key component that is critical for establishment of all interactions. This study only confirmed the key role of IdeR in *Mtb* as well as the importance of this protein as drug target, and no inhibitors were studied (16).

Due to production facility from point of view of the synthetic procedure (solid phase technique) and structure variation using of this kind of compounds for discovery of new drugs is common, in spite of instability of peptide compounds in biological media (17–19).

To assess the effectiveness of infected cells by *Mtb*, our constructs should be challenged *in vivo*. However, we defined two constructs that act as lead constructs which worth for more evaluations.

Conclusion

Whereas the ten of designed constructs showed potent results, in terms of computation and DNA binding energy, but only two of them could inhibit bacterial growth in the medium. Other factors that can affect the potency of drugs are cellwall transporting and chemical stability in the medium during culturing. The synthetic peptides are usually unstable in culture medium because of hydrolyzing of the amide bond. It can be accelerated by passing more time and temperature elevating (herein the culturing was down during one week at 37 °C). This could be a rational reason why the MIC of the synthetic amides is high.

The structure of the effective peptides (RPR and GVPG) can lead us to design new compounds by using of structure based searching method with high cell wall permeability and stability in biological medium.

Acknowledgment

The authors would thank Vice Chancellor of Health of Mashhad University of Medical Sciences for permission to use their laboratory in this study. The results described in this paper were part of PhD student thesis, Himen Salimizand, and supported by grant No 930710 from Mashhad University of Medical Sciences.

References

1. World Health Organization (WHO). Global Tuberculosis Report. 2015. Available at: http://www.who.int/tb/publications/global_report/en/.
2. Matsumoto M, Hashizume H, Tomishige T, Kawasaki M, Tsubouchi H, Sasaki H, *et al.* OPC-67683, a nitro-dihydro-imidazooxazole derivative with promising action against tuberculosis *in vitro* and in mice. *PLoS Med* 2006; 3:e466.
3. Cole ST, Alzari PM. Microbiology. TB- a new target, a new drug. *Science* 2005; 307:214–215.
4. Chung BK-S, Dick T, Lee D-Y. In silico analyses for the discovery of tuberculosis drug targets. *J Antimicrob Chemother* 2013; 68:2701–2709.
5. Rodriguez GM, Voskuil MI, Gold B, Schoolnik GK, Smith I. ideR, an essential gene in mycobacterium tuberculosis: role of ideR in iron-dependent gene expression, iron metabolism, and oxidative stress response. *Infect Immunol* 2002; 70:3371–3381.
6. Pandey R, Rodriguez GM. IdeR is required for iron homeostasis and virulence in Mycobacterium tuberculosis. *Mol Microbiol* 2014; 91:98–109.
7. Keyer K, Imlay JA. Superoxide accelerates DNA damage by elevating free-iron levels. *Proc Natl Acad Sci U S A* 1996; 93:13635–13640.
8. Wisedchaisri G, Chou CJ, Wu M, Roach C, Rice AE, Holmes RK. Crystal structures, metal activation, and DNA-Binding properties of two-domain ideR from Mycobacterium tuberculosis. *Biochemistry* 2007; 46:436–447.
9. El-Ayaan U, Abdel-Aziz AA, Al-Shihry S. Solvatochromism, DNA binding, antitumor activity and molecular modeling study of mixed-ligand copper(II) complexes containing the bulky ligand: Bis[N-(p-tolyl)imino]acenaphthene. *Eur J Med Chem* 2007; 42:1225–1233.
10. Mcalpine B. A colorimetric microassay for the detection of agents that interact with DNA. *1992*; 55: 1582–1587.
11. Bronstein JC, Weber PC. A Colorimetric Assay for high-throughput screening of inhibitors of herpes simplex virus Type 1 alkaline nuclease. *Anal Biochem* [Internet] 2001; 293:239–245.
12. Franzblau SG, Witzig RS, McLaughlin JC, Torres P, Madico G, Hernandez A, *et al.* Rapid, low-technology MIC determination with clinical Mycobacterium tuberculosis isolates by using the microplate Alamar

Blue assay. *J Clin Microbiol* 1998; 36:362–366.

13. Livak KJ, Schmittgen TD. Analysis of relative gene expression data using real-time quantitative PCR and the 2(-Delta Delta C(T)) Method. *Methods* 2001; 25:402–408.

14. Schwyn B, Neilands JB. Universal chemical assay for the detection and determination of siderophores. *Anal Biochem* 1987; 160:47–56.

15. Dragset MS, Poce G, Alfonso S, Padilla-Benavides T, loerger TR, Kaneko T, *et al.* A novel antimycobacterial compound acts as an intracellular iron chelator. *Antimicrob Agents Chemother* 2015; 59:2256–2264.

16. Ghosh S, Prasad KVS, Vishveshwara S, Chandra N. Rule-based modelling of iron homeostasis in

tuberculosis. *Mol Biosyst* 2011; 7:2750–2768.

17. Hao G, Rongji D, Kui Q, Zhongqiu T, Heyao W. A synthetic peptide derived from NK-lysin with activity against mycobacterium tuberculosis and its structure-function relationship. *Int J Pept Res Ther* 2011; 17:301–306.

18. Flexner C. HIV drug development: the next 25 years. *Nat Rev Drug Discov* 2007; 6:959–966.

19. Lau QY, Choo XY, Lim ZX, Kong XN, Ng FM, Ang MJY, *et al.* A head-to-head comparison of the antimicrobial activities of 30 ultra-short antimicrobial peptides against staphylococcus aureus, pseudomonas aeruginosa and Candida albicans. *Int J Pept Res Ther* 2015; 21:21–28.